Available online at www.sciencedirect.com
SCIENCE DIRECT®
Inorganica Chimica Acta 357 (2004) 95–102
Inorganica Chimica Acta
www.elsevier.com/locate/ica

Crystal structure, DNA-binding ability and cytotoxic activity of platinum(II) 2,2′-dipyridylamine complexes

Chao Tu [a], Xuefeng Wu [b], Qin Liu [a], Xiaoyong Wang [a], Qiang Xu [b], Zijian Guo [a,*]

[a] State Key Laboratory of Coordination Chemistry, Coordination Chemistry Institute, Nanjing University, 210093 Nanjing, PR China
[b] State Key Laboratory of Pharmaceutical Biotechnology, Nanjing University, 210093 Nanjing, PR China

Received 27 April 2003; accepted 14 June 2003

Abstract

Two platinum(II) complexes, [Pt(dpa)Cl_2] (**1**) and [Pt(dpa)CBDCA] (**2**), where DPA = 2,2′-dipyridylamine and CBDCA = 1,1-cyclobutanedicarboxylate, were synthesized and characterized by elemental analysis, IR spectroscopy, ES-MS and X-ray diffraction. Intermolecular hydrogen bonds were observed in both complexes (N–H···Cl for complex **1** and N–H···O for complex **2**), which may play a role in formation of hydrogen bonding in metal–DNA adducts. Complex **2** adopts a boat conformation so that the cyclobutane ring and bipyridyl groups are on the same side of the platinum square. The interactions of complexes **1** and **2** with DNA were studied by UV and Fluorescence Spectroscopy, which indicated that both complexes could interact with DNA through groove binding or intercalation. The in vitro cytotoxic activity against melanoma B16-BL6 cells and human Jurkat T-cells was also reported.

Keywords: Platinum(II) complex; 2,2′-Dipyridylamine; Crystal structure; DNA binding; Cytotoxic activity

1. Introduction

There is a huge scope in the design of novel Pt(II)-based anticancer complexes which possess improved clinical efficacy and undesired side effects [1–6]. One of the key strategies aimed at overcoming the drawbacks is to design platinum(II) complexes that interact with DNA in a different fashion from that of the currently used drugs [5,6]. Early structure–activity relationships (SAR) have defined the necessity of at least one NH moiety which is believed to be important for H-bonding interactions toward DNA [7], although the role of such NH groups is not completely clarified [8–11].

There is an increasing number of platinum compounds which contain no NH moiety but display significant antitumor activity [12–15]. Examples include Pt(II) complexes containing bipyridyl crown ethers, pyridine, bis(imidazole), bismethylimidazolecarbinol and 2-phenylpridine ligands. All these complexes have demonstrated certain degree of activity against tumor cell lines [12–15].

The 2,2′-dipyridylamine (DPA) is an aromatic amine sharing some similarity to 2,2′-bipyridine (BPY), however the central amine unit introduces several differences: the two pyridine rings of DPA are flexible in their coordination to metal centers, adopting either nearly coplanar or tilted pyridyl ring planes [16]. In contrast to the detailed studies on the platinum(II)–BPY complexes, little is known about the complexes of DPA ligand [17–19]. Pt(II) and Pd(II) complexes with the formulas of $[M^{II}(DPA)(AA)]$ and $[M^{II}(DPA)(pyc)]^+$ (AA, amino acid anion; pyc, pyridine-2-carboxylate; M^{II}, Pd^{II} and Pt^{II}) have been reported [18,19], and some of them have shown potential antitumor activity [18,19]. However, the structure of these complexes is unknown.

In this work, we have synthesized and structurally characterized in the solid state two Pt(II)–DPA complexes with both chloride or 1,1-cyclobutanedicarboxlate (CBDCA) as leaving groups (complexes **1** and **2**, shown in Fig. 1). The potential DNA-binding property of the complexes was investigated using the model

* Corresponding author. Tel.: +86-25-3594549; fax: +86-25-3314502.
E-mail address: zguo@netra.nju.edu.cn (Z. Guo).

0020-1693/$ - see front matter © 2003 Elsevier B.V. All rights reserved.
doi:10.1016/S0020-1693(03)00389-X

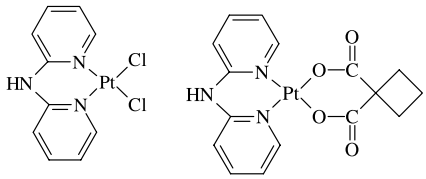

(1) (2)

Fig. 1. Schematic representation of [Pt(dpa)Cl_2] (**1**) and [Pt(dpa)CBDCA] (**2**).

compound guanosine-5′-monophosphate (5′-GMP) and calf thymus (CT) DNA. The cytotoxic activity against melanoma B16-BL6 cells and human Jurkat T-cells was also reported.

2. Experimental

2.1. Starting materials and physical methods

Solvents such as methanol and acetone were all analytical reagents and used as received. The $K_2[PtCl_6]$ was purchased from the First Reagent Factory of Shanghai, 2,2′-dipyridylamine (DPA) from Fluka, disodium salt of 5′-GMP and CT DNA from Sigma. The $K_2[PtCl_4]$ was synthesized by the reduction of $K_2[PtCl_6]$ using hydrazine following the standard procedure [20]. [Pt(dmso)$_2$$Cl_2$] and [Pt(dmso)$_2$CBDCA] were prepared according to the literature procedures [21,22].

The infrared spectra were recorded on a Bruker VECTOR22 spectrometer as KBr pellets (4000–500 cm^{-1}). Elemental analysis was performed on a Perkin–Elmer 240C analytical instrument.

Electrospray mass spectra were recorded using an LCQ electron spray mass spectrometer (ES-MS, Finnigan) by loading 1.0 μl of solution into the injection valve of the LCQ unit and then injecting into the mobile phase solution (50% of aqueous methanol) that was carried through the electrospray interface into the mass analyzer at a rate of 200 μl min^{-1}. The voltage employed at the electrospray needles was 5 kV, and the capillary was heated to 200 °C. A maximum ion injection time of 200 ms along with 10 scans was set. Positive and negative ion mass spectra were obtained. The predicted isotope distribution patterns for each of the complexes were calculated using the Isopro 3.0 program [23].

UV–Vis spectra were recorded on a UV-3100 spectrometer. Fluorescent spectra were recorded on a AMINCO Bowman Series 2 Luminescence Spectrometer.

2.2. Preparation of compounds

2.2.1. Pt(dpa)Cl_2 (*1*)

A solution of 0.171 g (1 mmol) DPA in 10 ml of methanol was added to a solution of 0.422 g (1 mmol) [Pt(dmso)$_2$$Cl_2$] in 50 ml methanol. The mixture was refluxed overnight and the solvent was removed under reduced pressure. The resulting [Pt(dpa)Cl_2] was washed three times with 20 ml water and 5 ml acetone and dried in vacuo. The yield was 0.355 g for compound **1** (81%). *Anal.* Calc. for $C_{10}H_9Cl_2N_3Pt$ (437.18): C, 27.47; H, 2.07; N, 9.61. Found: C, 27.51; H, 2.05; N, 9.59%. Selected IR data (cm^{-1}): 3474 (w), 3281 (s), 3088 (m), 1633 (s), 1584 (s), 1476 (s), 1234 (s), 766 (s), 533 (s). ES-MS *m*/*z*: 436 [M^-], 873 [2M]$^-$.

2.2.2. Pt(dpa)CBDCA (*2*)

This was synthesized in a way similar to **1**, and [Pt(dmso)$_2$$Cl_2$] was replaced by 0.493 g (1 mmol) of [Pt(dmso)$_2$CBDCA]. Yield: 83%. *Anal.* Calc. for $C_{16}H_{15}N_3O_4Pt$ (508.39): C, 37.80; H, 2.97; N, 8.27. Found: C, 37.82; H, 2.98; N, 8.28%. Selected IR data (cm^{-1}): 3473 (w), 3027 (m), 1654 (s), 1604 (m), 1487 (s), 1369 (s), 1116 (s), 765 (m), 535 (m). ES-MS *m*/*z*: 509 [M^+], 531 [M + Na^+], 1039 [2M + Na^+].

2.2.3. Pt(dpa)$(NO_3)_2$ (*3*)

To a suspension of 0.200 g (0.46 mmol) [Pt(dpa)Cl_2] in 15 ml water was added 0.153 g (0.9 mmol) $AgNO_3$. After the suspension has been stirred for 8 h at 50 °C in the dark, the solution was cooled to room temperature. The resulting AgCl precipitate was removed by centrifugation and the filtrate was lyophilized overnight.

2.3. Reaction of complex *3* with 5′-GMP

The [Pt(dpa)$(NO_3)_2$] with 2 mol equiv. of 5′-GMP (0.005 mmol) were added to 0.5 ml aqueous solution, the mixture was incubated at 37.8 °C in the dark for 24 h before the ES-MS spectra being recorded.

2.4. DNA-binding studies

Solutions of CT DNA in 50 mM NaCl/5 mM Tris–HCl (pH 7.3) gave a ratio of UV absorbance at 260 and 280 nm, A_{260}/A_{280}, of 1.8–1.9, indicating that the DNA was sufficiently free of protein [24]. Concentrated stock solution of DNA was prepared in 5 mM Tris–HCl/50 mM NaCl in water, pH 7.3, and the concentration of DNA was determined by UV absorbance at 260 nm after 1:100 dilutions. The molar absorption coefficient was taken as 6600 M^{-1} cm^{-1} [25]. Stock solutions were stored at 4 °C and used after no more than 4 days.

Complex **1** was dissolved in a mixed solution of 50% DMSO and 50% buffer (5 mM Tris–HCl/50 mM NaCl) at a concentration of 1.7×10^{-3} M and incubated for 2 h at room temperature before the DNA was added. The concentration of complex **1** was eventually reduced to 10^{-5} M while adding the calculated amounts of DNA (10^{-5} M, $r = 0.5$) and the final volume of the solutions were fixed to 3 ml. The UV–Vis spectra was recorded

after 0.5, 1.0, 1.5, 2.0, 2.5 and 3.0 h, respectively. It has been verified that the low DMSO percentage added to the DNA solution would not interfere with the nucleic acid [26].

The fluorescent spectra ($\lambda_{ex} = 526$ nm, $\lambda_{em} = 600$ nm) were also recorded at room temperature and the samples of complexes **1** and **2** were prepared in a similar way described above. The experiments were carried out by titrating the solution of platinum complexes (20 μl per scan) to the samples containing 2.45×10^{-5} M of DNA and 2.45×10^{-5} M EB (ethidium bromide).

2.5. Cytotoxicity assays

Melanoma B16-BL6 tumor cells and human Jurkat T-cells were grown in RPMI 1640 medium supplemented with 10% freshly inactivated fetal calf serum (FCS) and antibiotics. The solutions of complexes **1** and **2** were freshly prepared with the RPMI 1640 medium, and diluted to the required concentration with culture medium when used. The cells harvested from exponential phase were planted equivalently into a 96-well plate (2×10^5 per ml, 100 μl per well); then the compounds studied were added in a concentration gradient to give final concentrations at 1×10^{-4}, 1×10^{-5}, 1×10^{-6}, 1×10^{-7} and 1×10^{-8} M, respectively. The plates were kept at 37 °C in a humidified atmosphere of 5% CO_2 and incubated for 72 h respectively; then MTT [3-(4,5-dimethyl-2-thiazolyl)-2,5-diphenyl-2H-tetrazolium bromide] solution of an appropriate concentration (2 mg/ml) was added to each well (40 μl) and the plates incubated at 37 °C for 4 h. The measurements of absorbance of the solutions related to the number of live cells were performed on an ELISA spectrophotometer at 540 nm [27].

2.6. Crystallization

Crystallization of [Pt(dpa)Cl_2] and [Pt(dpa)CBDCA] were achieved by slow evaporation of their mother solution. After 3 days, yellow crystals (for compound **2**, colorless) suitable for X-ray structure analysis were obtained.

2.7. Crystal structure determination

The raw data of complexes **1** and **2** were collected on a Siemens SMART CCD diffractometer. Reflection data were measured at 20 °C using graphite monochromated Mo Kα ($\lambda = 0.71073$ Å) radiation with a detector distance of 4 cm and swing angle of −35°. The collected data were reduced using the program SAINT [28] and empirical absorption correction was carried out using SADABS [29] program. The structure was solved by direct methods that revealed the position of all non-hydrogen atoms and refined using the full-matrix least-squares method on F^2_{obs} by using the SHELXTL [30] software package. All non-H atoms were anisotropically refined. The molecular graphics were created using SHELXTL. Atomic scattering factors and anomalous dispersion correction were taken from the International Table for X-ray Crystallography [31].

3. Results and discussion

3.1. X-ray structure of complexes *1* and *2*

The crystal data, data collection, structural solution and refinement parameters for complexes **1** and **2** are summarized in Table 1. Selected bond distances and angles are listed in Tables 2 and 3, respectively.

Fig. 2 shows an ellipsoid plot with the numbering scheme of the complex **1**. The platinum is square-planar and coordinated by two nitrogen atoms from the chelating bidentate ligand (DPA) and two chloride atoms. The mean deviation from the best PtN_2Cl_2 plane is 0.0167 Å. The average Pt–Cl distance is 2.2968 Å (Pt1–Cl1 2.3010 Å; Pt1–Cl2 2.2925 Å). The bond length of Pt–N is in the expected region for a Pt(II)–pyridyl nitrogen bond [32]. In the coordination sphere all angles are near the idealized value of 90°. The largest deviation appears for the angle N2–Pt1–N3 which is 88.68(18)°. The angle of C1–N1–C6 is 127.3(5)° and the dihedral angle between the two best least-squares planes through the two pyridyl rings amounts to 147.6°. Intermolecular hydrogen bonds (N–H···Cl, symmetry code $[x - 1/2, -y + 1/2, z - 1/2]$) were observed in the crystal, with the hydrogen bond length being 2.421 Å. The angle between N–H···Cl is 168.77°.

As can be seen from Fig. 3, the platinum in complex **2** is coordinated by two equivalent pyridyl nitrogen atoms [N2 and N3] of DPA and two carboxyl oxygen atoms [O5 and O6] of CBDCA. The Pt(II) has the expected square planar geometry exhibiting the usual structure parameters. The mean deviation of the best PtN_2O_2 plane is 0.0296 Å. The CBDCA ligand displays similar features to those described in the literature [33–36]. The two six-membered chelate rings which the ligand DPA and CBDCA formed with the Pt(II) atom adopts the boat conformation (Fig. 4) and the cyclobutane ring is nearly perpendicular to the Pt(II) coordination plane. The cyclobutane ring can adopt either a planar geometry or can have a puckered conformations. In the case of carboplatin, a large thermal parameters for C16 (0.101) was observed, which was attributed to the dynamic puckering between two conformations [37]. The angle of C1–N1–C6 is 130.3(8)° and the dihedral angle between the two best pyridyl rings is 159.2° which is 11.6° larger than that appeared in complex **1**. The bonds lengths between Pt(II) and oxygen atoms of CBDCA, in

Table 1
Crystal data and structure refinement for complexes **1** and **2**

	Complex **1**	Complex **2**
Empirical formula	$C_{10}H_9Cl_2N_3Pt$	$C_{16}H_{15}N_3O_4Pt$
Formula weight	437.19	508.40
Temperature (K)	293(2)	293(2)
Crystal size (mm)	$0.20 \times 0.18 \times 0.18$	$0.18 \times 0.16 \times 0.15$
Crystal habit/color	block/yellow	block/colorless
Crystal system	monoclinic	triclinic
Space group	$P2(1)/n$	P-1
a (Å)	9.9720(11)	9.1181(15)
b (Å)	10.1771(12)	9.6844(17)
c (Å)	1.7846(13)	10.0948(17)
α (°)	90	68.377(3)
β (°)	94.239(2)	67.353(3)
γ (°)	90	70.401(3)
V (Å^3)	1192.7(2)	745.1(2)
Z	4	2
Calculated density (Mg m^{-3})	2.435	2.266
Absorption coefficient (mm^{-1})	12.186	9.444
$F(000)$	808	484
θ range for data collection (°)	2.58–27.06	2.27–28.07
Limiting indices	$-10 \leqslant h \leqslant 12$, $-13 \leqslant k \leqslant 10$, $-15 \leqslant l \leqslant 13$	$-11 \leqslant h \leqslant 12$, $-12 \leqslant k \leqslant 10$, $-13 \leqslant l \leqslant 13$
Reflections collected	6687	4524
Independent reflections	2589	3339
Absorption correction	empirical	empirical
Data/restraints/parameters	2589/0/145	3339/0/217
Goodness-of-fit on F^2	0.970	0.941
R_{int}[a]	0.0410	0.0361
Final R indices $[I > 2\sigma(I)]$	$R_1 = 0.0326$[b], $wR_2 = 0.0736$[c]	$R_1 = 0.0477$, $wR_2 = 0.0873$
R indices (all data)	$R_1 = 0.0387$, $wR_2 = 0.0750$	$R_1 = 0.0638$, $wR_2 = 0.0904$
Largest difference peak and hole (e Å^3)	2.815 and −1.614	2.967 and −1.642

[a] $R_{int} = \sum |F_o^2 - F_o^2(\text{mean})| / \sum [F_o^2]$.
[b] $R = \sum ||F_o| - |F_c|| / \sum |F_o|$.
[c] $R_w = [\sum w(|F_o| - |F_c|)^2 / \sum w(|F_o|)^2]^{1/2}$.

Table 2
Selected bond lengths (Å) and angles (°) of complex **1**

Bond lengths	
Pt(1)–N(2)	2.010(4)
Pt(1)–N(3)	2.012(4)
Pt(1)–Cl(2)	2.2925(15)
Pt(1)–Cl(1)	2.3010(15)
Bond angles	
N(2)–Pt(1)–N(3)	88.68(18)
N(2)–Pt(1)–Cl(2)	177.35(12)
N(3)–Pt(1)–Cl(2)	90.87(14)
N(2)–Pt(1)–Cl(1)	90.95(13)
N(3)–Pt(1)–Cl(1)	177.02(13)
Cl(2)–Pt(1)–Cl(1)	89.37(6)
C(6)–N(1)–C(1)	127.3(5)

complex **2**, are 2.005(6) Å [Pt1–O2] and 2.011(6) Å [Pt1–O1], respectively.

The intermolecular hydrogen bonds (N–H···O, symmetry code $[x, y-1, z]$) are also found in the crystal of complex **2**, the hydrogen bond length is 2.163 Å and the angle between N–H···O is 139.54°.

3.2. ES-MS study

The ES-MS spectrum for the reaction of complex **3** with 2 mol equiv. of 5′-GMP was recorded after 24 h at 37.8 °C in aqueous solution (Fig. 5). As can be seen from Fig. 5, apart from some unreacted 5′-GMP which give rise to peaks at 724.9 $[2GMP]^-$ and 746.9 $[2GMP + Na]^-$, the major peaks at 1088.8 and 1452.7 can be assigned to $[Pt(dpa)(GMP)_2]^-$ and $[Pt(dpa)(GMP)_2 + GMP]^-$. The calculated molecular masses and the isotopic distribution of these peaks matched perfectly with the corresponding formulas. The formation of $[Pt(dpa)(GMP)_2 + GMP]^-$ may be due to the high temperature and pressure in the capillary of the spectrometer, and similar association of GMP has been observed previously [32].

3.3. UV monitored time-dependent reaction of complex *1* with CT DNA

The time-dependent absorption spectra of complex **1** (2.27×10^{-5} M) in the absence and presence of CT DNA

Table 3
Selected bond lengths (Å) and angles (°) of complex **2**

Bond lengths	
Pt(1)–N(2)	1.978(7)
Pt(1)–N(3)	1.997(7)
Pt(1)–O(2)	2.005(6)
Pt(1)–O(1)	2.011(6)
O(1)–C(11)	1.291(11)
O(2)–C(12)	1.327(11)
O(3)–C(11)	1.209(10)
O(4)–C(12)	1.220(11)
C(13)–C(15)	1.560(13)
C(13)–C(14)	1.559(12)
C(14)–C(16)	1.500(14)
C(15)–C(16)	1.510(15)
Bond angles	
N(2)–Pt(1)–N(3)	91.4(3)
N(2)–Pt(1)–O(2)	177.1(3)
N(3)–Pt(1)–O(2)	90.3(3)
N(2)–Pt(1)–O(1)	88.6(3)
N(3)–Pt(1)–O(1)	178.3(3)
O(2)–Pt(1)–O(1)	89.8(3)
C(11)–O(1)–Pt(1)	122.8(6)
C(12)–O(2)–Pt(1)	121.4(6)
C(6)–N(1)–C(1)	130.3(8)
C(1)–N(2)–Pt(1)	123.9(6)
C(5)–N(2)–Pt(1)	120.8(6)
C(6)–N(3)–Pt(1)	122.5(6)
C(10)–N(3)–Pt(1)	118.2(6)
C(15)–C(13)–C(14)	88.4(7)
C(16)–C(14)–C(13)	89.7(8)
C(16)–C(15)–C(13)	89.3(8)
C(14)–C(16)–C(15)	92.5(8)

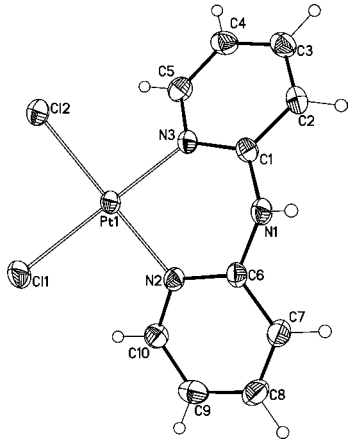

Fig. 2. Molecular structure and labeling of complex **1**. Ellipsoids are drawn at the 30% probability level.

$(5.67 \times 10^{-5}$ M) is shown in Fig. 6. It is interesting to find that the intensity of the absorption band at 301.5 nm which is attributed to the metal to the ligand charge transfer absorption (MLCT) does not change significantly with the time while the absorption around 272 nm increased dramatically upon addition of CT DNA until it reached a plateau after 3 h and a new band at 283 nm appeared. This phenomenon can be an indication of the

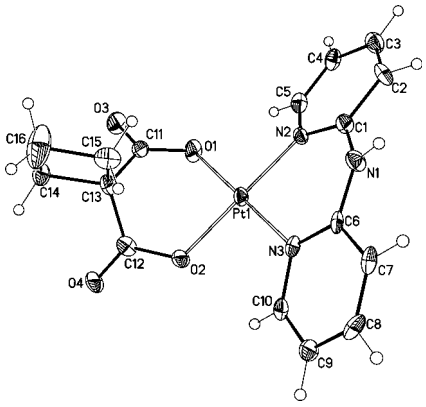

Fig. 3. Molecular structure and labeling of complex **2**. Ellipsoids are drawn at the 30% probability level.

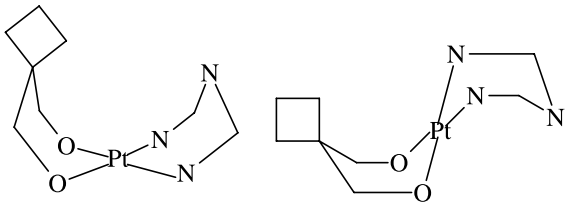

Fig. 4. Two possible relative orientations for the CBDCA and the dpa ligand in complex **2**. The conformation on the left (*cis*) is adopted in complex **2**.

interaction between complex **1** and DNA. A similar behavior was previously observed for copper complexes [38–40], where the hyperchromism was attributed to the dissociation of ligand aggregates and the breakage of intermolecular hydrogen bonds when bound to DNA. The exact mode of interaction remains to be defined. Complex **2** does not show significant time-dependent changes in the presence of DNA.

3.4. Fluorescence spectroscopic studies

The fluorescent emission of EB bound to DNA in the absence and the presence of complexes **1** and **2** are shown in Fig. 7. The emission band at 600 nm of the DNA–EB system decreased in intensity with the increase of the concentration of the two Pt(II) complexes, which indicated that the complexes can replace EB from the DNA–EB system. Such a characteristic change is often observed in the intercalative DNA interaction [40]. The data suggest that intercalation may be an alternative binding mode for complexes **1** and **2** due to the planarity of the DPA rings.

3.5. Cytotoxic activity

The effects of both complexes **1** and **2** on Melanoma B16-BL6 tumor cells and human Jurkat T-cells

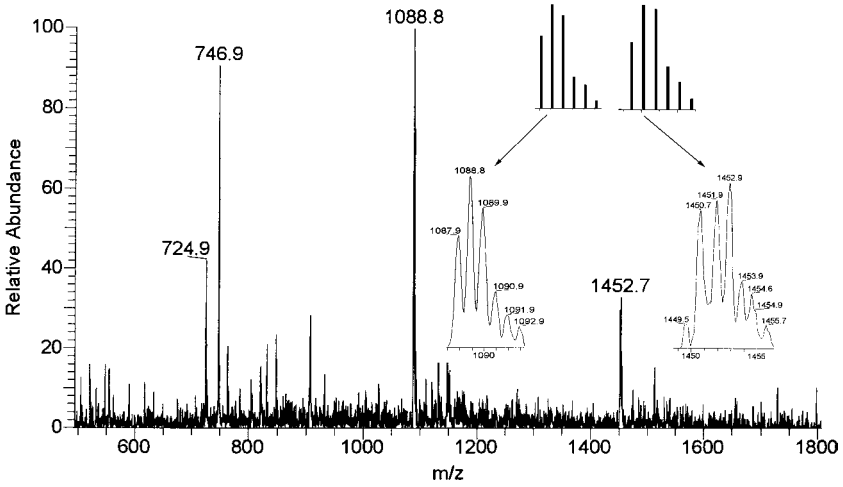

Fig. 5. The ES-MS spectrum showing the reaction adducts of complex **4** with 5′-GMP. The peaks at 1088.8 and 1452.7 were assigned to $[Pt(dpa)(GMP)_2]^-$ and $[Pt(dpa)(GMP)_2 + GMP]^-$, respectively. The solid line peaks on top right corner are calculated peaks for the two species.

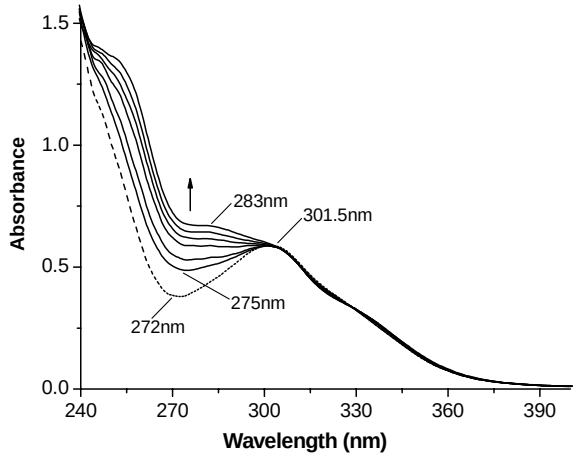

Fig. 6. Time-dependent absorption spectra of complex **1** (5.7×10^{-5} mol l^{-1}) in the absence (dashed line) and presence (solid lines, represent 0.5, 1, 1.5, 2, 2.5 and 3 h, respectively) of a fixed amount of CT DNA (2.3×10^{-5} mol l^{-1}) at room temperature.

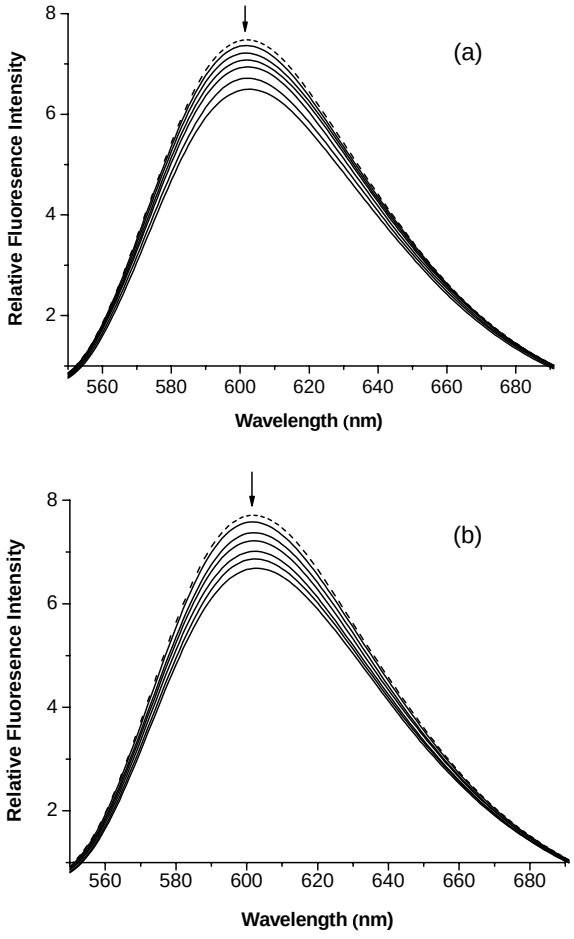

Fig. 7. Fluorescence emission spectra (excited at 526 nm) of EB bound to CT DNA in the absence (dashed line) and presence (solid lines) of increasing amounts of 1.7×10^{-3} mol l^{-1} complex **1** (**a**) and 1.48×10^{-3} mol l^{-1} complex **2** (**b**) (20 μl per scan).

proliferation after 72 h are reported in Fig. 8. Both complexes exhibited considerable inhibition rates only at high concentration (10^{-4} M). The change of leaving groups (chloride or CBDCA) had no impact on the activity. The data should be interpreted with care because at such a high concentration the cytotoxic effect of the solvent (for **1**, 0.67% DMSO; for **2**, 1% DMF) began to become relevant.

4. Conclusion

This work provided two of the very few crystal structures of Pt(II)–DPA complexes. It is shown that changing the leaving group (chloride or CBDCA) on Pt(II)–DPA system had little impact on the ring conformation of DPA. The pyridyl amine proton in complexes **1** and **2** may favor their hydrogen bonding to DNA and thus stabilizes the metal–DNA adducts [18,19]. The DNA-binding mode of these complexes is

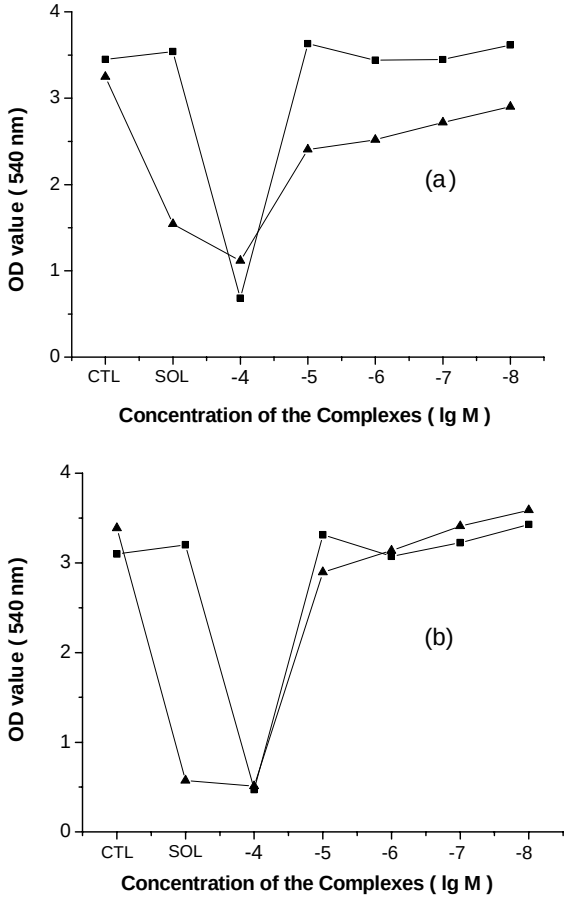

Fig. 8. Cytotoxic activity of complexes **1** (■) and **2** (▲) against selected tumor cell lines: Melanoma B16-BL6 tumor cells (a) and human Jurkat T-cells (b). The solvent contains the maximum concentration of DMSO/DMF used to dissolve tested compounds.

currently uncertain, spectroscopic data suggest that the compounds may be able to interact with DNA by groove binding or intercalation, although ES-MS study indicated the formation of covalent binding adduct of complex **1** and 5′-GMP. The in vitro tests show that the cytotoxicity of these complexes against Melanoma B16-BL6 tumor cells and human Jurkat T-cells does not warrant further biological testing. We are currently carrying out studies on other novel heterocyclic Pt(II) complexes so as to find more active species of the type.

Acknowledgements

We are grateful for the financial support of the National Natural Science Foundation of China (Grant Nos. 29925102, 20231010 and 20228102).

References

[1] B. Lippert (Ed.), Cisplatin: Chemistry and Biochemistry of a Leading Anticancer Drug, Wiley-VCH, Weinhein, 1999.
[2] J. Reedijk, Chem. Commun. (1996) 801.
[3] Y. Kidani, K. Inagaki, R. Saito, S. Tsukagoshi, J. Clin. Hematol. Oncol. 7 (1977) 197.
[4] V. Boudny, O. Vrana, F. Gaucheron, V. Kleinwachter, M. Leng, V. Brabec, Nucleic Acids Res. 20 (1992) 267.
[5] Z. Guo, P.J. Sadler, Angew. Chem., Int. Ed. Engl. 38 (1999) 1512.
[6] E. Wong, C.M. Giandomenico, Chem. Rev. 99 (1999) 2451.
[7] J. Reedijk, Inorg. Chim. Acta 198 (1992) 873.
[8] G. Admiraal, J.L. van der Veer, R.A.G. de Graaff, J.H.J. den Hartog, J. Reedijk, J. Am. Chem. Soc. 109 (1987) 592.
[9] S.E. Sherman, D. Gibson, A.H. Wang, S.J. Lippard, J. Am. Chem. Soc. 110 (1988) 7368.
[10] S.T. Sullivan, A. Ciccarese, F.P. Fanizzi, L.G. Marzilli, J. Am. Chem. Soc. 38 (2001) 9345.
[11] M.J. Bloemink, R.J. Heetebrij, K. Inagaki, Y. Kidani, J. Reedijk, Inorg. Chem. 31 (1992) 4656, and references therein.
[12] A. Gund, B.K. Keppler, Angew. Chem., Int. Ed. Engl. 33 (1994) 186.
[13] L.K. Webster, G.B. Deacon, D.P. Buxton, B.L. Hillcoat, A.M. James, I.A.G. Roos, R.J. Thomson, L.P.G. Wakelin, T.L. Williams, J. Med. Chem. 35 (1992) 3349.
[14] M.J. Bloemink, H. Engelking, S. Karentzpoulos, B. Krebs, J. Reedijk, Inorg. Chem. 35 (1996) 619.
[15] T. Okada, I.M. El-Mehasseb, M. Kodaka, T. Tomohiro, K. Okamoto, H. Okuno, J. Med. Chem. 44 (2001) 4661.
[16] R.E. Shepherd, Y. Chen, R.A. Kortes, M.S. Ward, Inorg. Chim. Acta 303 (2000) 30.
[17] R. Romeo, N. Nastasi, L.M. Scolaro, M.R. Plutino, A. Albinati, A. Macchioni, Inorg. Chem. 37 (1998) 5460, and references therein.
[18] A.K. Paul, H. Mansuri-Torshizi, T.S. Srivastava, S.J. Chavan, M. Chitnis, J. Inorg. Biochem. 50 (1993) 9.
[19] A.K. Paul, T.S. Srivastava, S.J. Chavan, M.P. Chitnis, S. Desai, K.K. Rao, J. Inorg. Biochem. 61 (1996) 179.
[20] G.B. Kaufmann, D.O. Cowan, Inorg. Synth. 7 (1963) 240.
[21] J.H. Price, A.N. Williamson, R.F. Shramm, B.B. Wayland, Inorg. Chem. 11 (1972) 1280.
[22] P. Bitha, G.O. Morton, T.S. Dunne, E.F. Delos Santos, Y. Lin, S.R. Boone, R.C. Haltiwanger, C.G. Pierpont, Inorg. Chem. 29 (1990) 645.
[23] J.A. Yergey, Int. J. Mass Spec. Ion Phys. 52 (1983) 337.
[24] J. Marmur, J. Mol. Biol. 3 (1961) 208.
[25] M.E. Reichmann, S.A. Rice, C.A. Thomas, P. Doty, J. Am. Chem. Soc. 76 (1954) 3047.
[26] M. Baldini, M. Belicchi-Ferrai, F. Bisceglie, G. Pelosi, S. Pinelli, P. Tarasconi, Inorg. Chem. 42 (2003) 2049.
[27] T. Mosmann, Immunol. Methods 65 (1983) 55.
[28] G.M. Sheldrick, SAINT v4 Software Reference Manual, Siemens Analytical X-Ray Systems, Madison, WI, 1996.
[29] G.M. Sheldrick, SADABS, Program for Empirical Absorption Correction of Area Detector Data, University of Gottingen, Germany, 1996.
[30] G.M. Sheldrick, SHELXTL, v5 Reference Manual, Siemens Analytical X-Ray Systems, Madison, WI, 1996.
[31] A.J. Wilson, International Table for X-Ray Crystallography, vol. C, Kluwer Academic Publishers, Dordrecht, 1992 (Tables 6.1.1.4 (p.500) and 4.2.6.8 (p.219), respectively).
[32] Z. Guo, A. Habtemariam, P.J. Sadler, R. Palmer, B.S. Potter, New J. Chem. 22 (1998) 11.
[33] J.Y. Zhang, Q. Liu, C. Duan, Y. Shao, J. Ding, Z. Miao, X.-Z. You, Z. Guo, J. Chem. Soc., Dalton Trans. (2002) 591.
[34] M.S. Ali, J.H. Thurston, K.H. Whitmire, A.R. Khokhar, Polyhedron 21 (2002) 2659.
[35] A.D.Q. Ferreira, A. Bino, D. Gibson, Inorg. Chim. Acta 265 (1997) 155.
[36] S. Neidle, I.M. Ismail, P.J. Sadler, J. Inorg. Biochem. 13 (1980) 205.

[37] B. Beagley, D.W.J. Cruickshank, C.A. McAuliffe, R.G. Pritchard, A.M. Zaki, R.L. Beddoes, R.J. Cernik, O.S. Mills, J. Mol. Struct. 130 (1985) 97.
[38] F. Liu, K.A. Meadows, D.R. McMillin, J. Am. Chem. Soc. 115 (1993) 6699.
[39] J. Liu, T.X. Zhang, T.B. Lu, L.H. Qu, H. Zhou, Q.L. Zhang, L.N. Ji, J. Inorg. Biochem. 91 (2002) 269.
[40] C.V. Kumar, J.K. Barton, N.J. Turro, J. Am. Chem. Soc. 107 (1985) 5518.